

# Heavy Ions at LHC: Theoretical Issues

R. J. Fries<sup>1</sup>, B. Müller<sup>1</sup>

Department of Physics, Duke University, Durham, NC 27708  
e-mail: rjfries@phy.duke.edu

**Abstract.** We give a brief overview of our current theoretical understanding of ultra-relativistic heavy ion collision and the properties of super-hot nuclear matter. We focus on several issues that have been discussed in connection with experimental results from the CERN SPS and from the Relativistic Heavy Ion Collider RHIC. We give an extrapolation of our current knowledge to LHC energies and ask which physics questions can be addressed at the LHC.

PACS: 24.85.+p, 25.75.Nq, 13.85.-t

---

## 1 Introduction

The ALICE detector at LHC will be the next generation facility for exploring the features of hot nuclear matter. The goal is to learn more about the universe as it existed a few microseconds after the big bang. A very hot and dense phase of partons was present at these times. Later, a phase transition occurred during which hadronic matter as we know it today was formed. In the laboratory we try to create conditions that are similar to those in the early universe by colliding ultrarelativistic heavy ions, e.g. at the RHIC facility and — in a few years from now — at the LHC. The hope is to create a deconfined quark gluon plasma (QGP) for a few fm/c and to study its properties. Fig. 1 shows our knowledge about QCD in the plane of temperature  $T$  and baryon chemical potential  $\mu_B$  with points that were tested in heavy ion experiments so far. Also the region covered by the LHC, which lies at small baryon chemical potential but at temperatures well above the phase transition temperature of  $T_c \sim 170$  MeV [1] is shown.

The theoretical knowledge about the QCD phase transition so far is mainly coming from lattice QCD (see e.g. [2] for a review). It is possible to simulate the behavior of QCD along the  $T$ -axis for  $\mu_B = 0$ . It is found that the scaled energy density  $\epsilon/T^4$  steeply increases at  $T_c$ . Since

$$\epsilon = g_{\text{DOF}} \frac{\pi^2}{30} T^4, \quad (1)$$

this can be understood by the rapidly rising number of degrees of freedom  $g_{\text{DOF}}$  when the confined partons are liberated. Lattice QCD also shows that the deconfinement phase transition occurs together with a restoration of the spontaneously broken chiral symmetry. Recently calculations at finite  $\mu_B$  became available [3]. They predict a critical point on the phase transition line that is shown in Fig. 1.

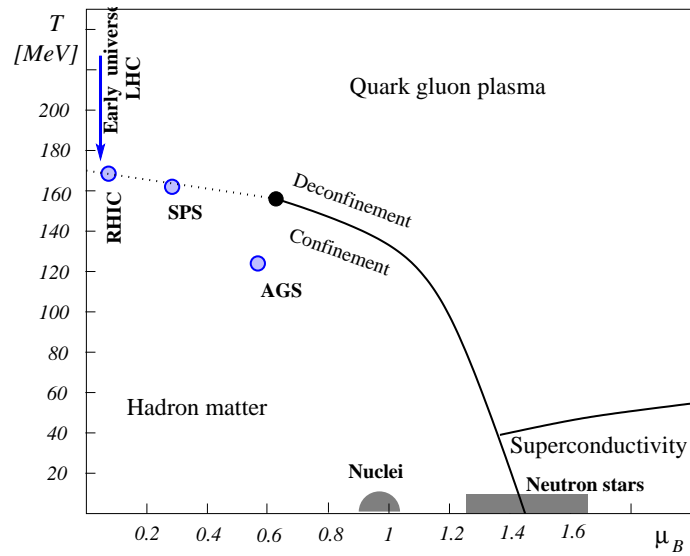


**Fig. 1.** Schematic QCD phase diagram in the  $T - \mu_B$  plane. At low  $T$  and  $\mu_B$  nuclear matter shows confinement and hadrons are the degrees of freedom. At higher  $T$  a phase transition to a deconfined quark gluon plasma with restored chiral symmetry is predicted by lattice QCD. The phase transition might exhibit a critical point at about  $\mu_B \sim 700$  MeV. More exotic quark phases can occur at high density, e.g. in the interior of very dense neutron stars. Chemical freeze-out conditions reached in heavy ion experiments at AGS, SPS and RHIC are also indicated. The blue arrow along the  $T$  axis shows how the matter is supposed to evolve at LHC before freeze-out, starting at very high temperature. The evolution of the early universe a few microseconds after the big bang took a similar path.

## 2 Signatures of the phase transition

If a quark gluon plasma is created in a collision of two large nuclei, it eventually has to hadronize again. The detectors in our experiments can only measure the hadronic debris from this collision. A direct observation of the plasma is not possible. There has been a long discussion over the past 25 years what the possible signatures of a phase transition from a quark gluon plasma might be. We give a short (and probably incomplete) list of some of the more popular ideas:

- Indirect measurements of thermodynamical quantities like the latent heat of the phase transition.
- The enhanced production of strange particles.
- Modifications of hadron properties, like the mass and width of the  $\rho$  meson, through the presence of hot nuclear matter.
- The detection of thermal photon or dilepton radiation from a thermalized QGP.
- The suppression of quarkonia like the  $J/\Psi$ .
- The energy loss of fast partons in a QGP, the so called jet quenching.
- Fluctuations in net charge or baryon number.
- Collective vacuum excitations like the disoriented chiral condensate (DCC).

In the following we discuss some of these ideas.

### 2.1 Latent heat

One of the simplest approaches one can think of is to measure quantities that are thermodynamically related to the phase transition, like the latent heat. A very interesting observation has been made regarding the slope of hadron spectra. Hadron spectra at low transverse momenta — below several GeV/c, can be described phenomenologically by a blast wave fit [4]. This assumes a thermalized spectrum with an effective temperature  $T$ . The spectrum is additionally boosted by a collective radial flow. The data collected for kaons at different energies seem to indicate that a plateau in the temperature was reached at SPS energies, while at higher RHIC energies the temperature is again rising. This could be interpreted as latent heat that is used to free the additional partonic degrees of freedom.

### 2.2 Strangeness enhancement

One of the classical signatures of the QGP is strangeness enhancement [5]. Since the strangeness content of the colliding nuclei in the initial state is nearly negligible, all strange particles in the final state have to be generated in the collision. In

purely hadronic matter, e.g. kaons and  $\Lambda$ s have to be produced through hadronic channels. In a quark gluon plasma,  $s\bar{s}$  pairs will be created. This is enhanced by the relatively small strange quark mass  $m_s < T_{\text{QGP}}$  in the chirally restored phase. The strange quarks will then hadronize into strange hadrons and lead to higher yields compared to the hadronic scenario. This can already be seen at the CERN SPS [6].

### 2.3 $J/\Psi$ suppression

It was argued by Matsui and Satz [7], that the disappearance of quarkonia states is a signal for the QGP. Lattice calculations show that the heavy quark potential is effectively screened in a plasma above  $T_c$ , so that  $c\bar{c}$  bound states are melting [8]. It is then unlikely that the  $c\bar{c}$  will find together at hadronization. Instead, they will mostly end up in open charm states. However, already at RHIC energies charm quarks could be so abundant, that spontaneous recombination of  $c\bar{c}$  pairs could occur if  $c$  quarks thermalize in the medium [9]. That would alter the suppression scenario and could even lead to a  $J/\Psi$  enhancement.

### 2.4 Jet quenching

Fast partons produced in hard QCD interactions between the two colliding nuclei have to travel through the hot and dense medium surrounding them. It was proposed very early by Bjorken [10], that these partons lose energy by interactions with the medium, see Fig. 2. This "jet quenching" was studied in a series of theoretical papers over the last 10 years [11]. The main process is the induced radiation of gluon bremsstrahlung by interactions with the hot nuclear matter. This results in a suppression of hadron production at  $P_T > 2$  GeV. Furthermore, since for strong energy loss the emission of high- $P_T$  hadrons is dominated by surface emission, the correlated backside jet nearly vanishes. This was confirmed at RHIC [12, 13]. Fig. 3 shows the nuclear suppression factor  $R_{AA}$  for pions which is defined as the particle yield in Au+Au collisions normalized by the yield in  $p + p$  collisions scaled by the number of binary nucleon-nucleon collisions. If a heavy ion collision were just a superposition of individual nucleon-nucleon collisions,  $R_{AA}$  would be 1. In recent  $d$ +Au control experiments, where no QGP is expected to be produced, indeed, no suppression in the hadron yield and back-to-back correlations similar to  $p + p$  collisions were found [14].

Theoretically, the effect of energy loss for hadron spectra can be described by medium modifications in the fragmentation function of a parton  $a$  into hadron  $h$  [15]. This modification approximately corresponds to a rescaling of the variable  $z$

$$D_{a \rightarrow h}(z, Q^2) \longrightarrow \tilde{D}_{a \rightarrow h}(z, Q^2) \approx D_{a \rightarrow h}\left(\frac{z}{1 - \Delta E/E}, Q^2\right). \quad (2)$$

Theory predicts that the energy loss is quadratically dependent on the length of the medium due to the so-called non-abelian Landau-Pomeranchuk-Migdal interference effect [16].

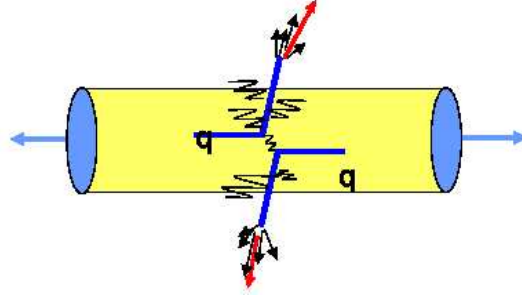


**Fig. 2.** The jet quenching mechanism: Partons produced in hard QCD processes suffer from final state interactions with the surrounding hot medium. Induced bremsstrahlung leads to energy loss.

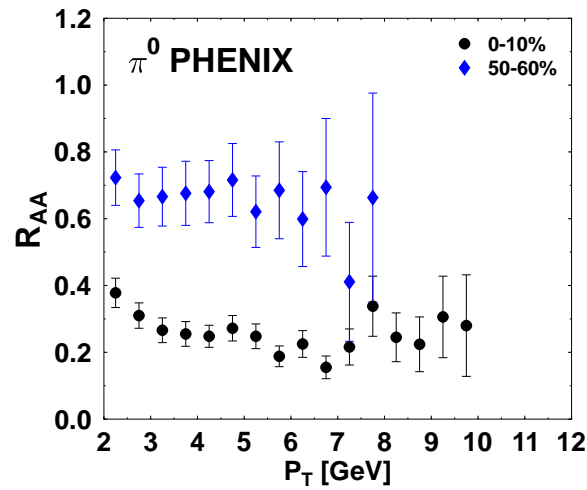


**Fig. 3.**  $R_{AA}$  for  $\pi^0$  measured by the PHENIX collaboration [13] in Au+Au collisions at RHIC for two different centrality bins. A large suppression can be observed for central collisions

### 3 Surprising RHIC results

Besides the search for standard QGP signatures and the confirmation of long standing theoretical expectations, experimental results from RHIC have provided many surprises. In this section we want to discuss the anomalous baryon enhancement and the elliptic flow pattern found at RHIC.

It was widely assumed that hadron production at RHIC for  $P_T > 2$  GeV can be described by perturbative QCD. This seemed to work well for pions if all known nuclear corrections, like shadowing and energy loss, are taken into account. On the other hand, protons and antiprotons deviate from this behavior. In a scenario with partonic energy loss, the suppression of  $p$  and  $\bar{p}$  should be the same as for pions. Furthermore, pQCD would predict a ratio  $p/\pi^0 < 0.2$ . RHIC results show that the  $p/\pi^0$  ratio is about 1 between 1.5 and 4.5 GeV/ $c$ , and that there is nearly no nuclear suppression in the yield of protons in this transverse momentum region [17]. A similar behavior was found in the strangeness sector for  $\Lambda$ s and kaons [18].

An important quantity that can be measured in heavy ion collisions is the azimuthal anisotropy. At nonzero impact parameter  $b > 0$ , the overlap zone of the two nuclei is not spherically symmetric. The initial anisotropy translates into an anisotropy of the final hadron spectra. This can be quantified by an expansion of the spectrum into harmonics

$$\frac{dN}{2\pi P_T dP_T d\phi} = \frac{dN}{2\pi P_T dP_T} (1 + v_1(P_T) \cos \phi + v_2(P_T) \cos 2\phi + \dots). \quad (3)$$

The coefficient  $v_2$  describes the elliptic anisotropy in the spectrum.  $v_2$  has been measured in RHIC experiments and shows a surprising dependence on the hadron species. As a function of  $P_T$  it rises and saturates above 2 GeV/ $c$ . The value of saturation is always larger for baryons compared to mesons [18]. It is believed that at these and higher values of  $P_T$  the mechanism for translating the initial anisotropy into a final one is again partonic energy loss. Partons going into a direction where the interaction zone is less extended will suffer less energy loss. However, this mechanism should be blind to the hadron species.

The results above suggest that the range of validity for leading twist perturbative QCD calculations only starts at higher transverse momentum. Instead, the baryon enhancement and the azimuthal flow pattern can be understood in a simple picture of parton recombination [19]. In pQCD hadronization happens through fragmentation. A single parton with momentum  $p$  splits into gluons and  $q\bar{q}$  pairs that eventually form hadrons. One of these hadrons is then measured and has momentum  $P = zp$ , ( $z < 1$ ). The hadron spectrum is given by

$$E \frac{dN_h}{d^3P} = \sum_a \int_0^1 \frac{dz}{z^2} D_{a \rightarrow h}(z) E_p \frac{dN_a}{d^3p} \quad (4)$$

where  $dN_a/d^3p$  is the spectrum of partons  $a$  and  $p = P/z$  is the parton momentum.

On the other hand, if phase space is already densely populated with partons, these can simply recombine to give mesons  $M$  and baryons  $B$

$$q\bar{q} \rightarrow M, \quad qqq \rightarrow B, \quad \bar{q}\bar{q}\bar{q} \rightarrow \bar{B}. \quad (5)$$

In this case, the momenta of the valence partons add up. Quantitatively this can be formulated in a coalescence formalism using hadron wave functions  $\phi_h$  in light cone coordinates [20]. For a meson  $M$  the spectrum can be written as

$$E \frac{dN_M}{d^3P} = C_M \int_{\Sigma} d\sigma \frac{P \cdot u(\sigma)}{(2\pi)^3} \int_0^1 dx w_q(\sigma; xP^+) |\phi_M(x)|^2 w_{\bar{q}}(\sigma; (1-x)P^+) \quad (6)$$

where  $C_M$  is a degeneracy factor,  $w_q$  and  $w_{\bar{q}}$  are the phase space distributions of the recombining quark and antiquark respectively,  $x$  is the momentum fraction of the quark in light cone coordinates and  $\Sigma$  is the hadronization hypersurface in Minkowski space.

It can be shown that recombination is always more effective than fragmentation for an exponential parton spectrum, but fragmentation will dominate at high  $P_T$  for a parton spectrum in power law form. Furthermore, for an exponential parton spectrum  $w = e^{-P^+/T}$ , we have

$$w_q(xP^+)w_{\bar{q}}((1-x)P^+) = e^{-P^+/T} \quad (7)$$

in the case of a meson  $M$  and analogously

$$w_q(x_1P^+)w_q(x_2P^+)w_q((1-x_1-x_2)P^+) = e^{-P^+/T} \quad (8)$$

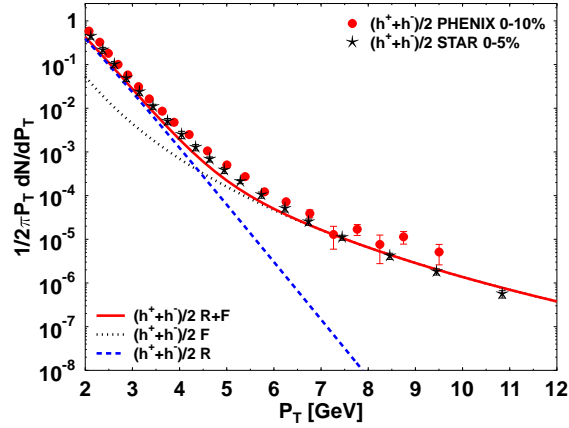
in the case of a baryon  $B$ .  $P^+$  here always denotes the large component of the hadron momentum on the light cone. Hence recombination naturally provides a ratio  $B/M \sim 1$ . We should add that the description of recombination given above is only valid if  $P^+$  is much larger than  $\Lambda_{\text{QCD}}$  and the masses of the hadrons.

Fig. 4 shows the result of a calculation for charged hadrons at RHIC using recombination from a thermalized phase of constituent quarks with a temperature  $T = 175$  MeV and an average radial flow velocity  $v_T = 0.55c$  and fragmentation in a leading order pQCD calculation including energy loss. One can clearly see the two different domains of hadron production. Only above  $P_T = 5$  GeV/ $c$  is leading twist pQCD a good description for hadron production. Below that recombination is important. Data on the  $p/\pi^0$  ratio in this momentum range are well reproduced by this calculation.

For the recombination of partons, one can derive a simple scaling law that connects the azimuthal anisotropy  $v_2$  for partons  $p$  and hadrons  $h$  [20, 23]

$$v_2^h(P_T) = n v_2^p(P_T/n) \quad (9)$$

where  $n = 2$  for mesons and  $n = 3$  for baryons. This scaling law which was recently confirmed by the STAR and PHENIX collaborations [24], can be considered as a new “smoking gun” for the creation of a quark gluon plasma. The scaling law visualizes the anisotropic flow in the parton phase before hadronization.



**Fig. 4.** The spectrum of charged hadrons  $(h^+ + h^-)/2$  at midrapidity for central Au+Au collisions at RHIC. The result of a leading order pQCD calculation with energy loss (dotted line), recombination of a thermalized parton phase (dashed line) and the sum of both (solid line) are shown. Data are from STAR [21] and PHENIX [22].

## 4 What's different at LHC?

At LHC lead nuclei will collide with a center of mass energy  $\sqrt{s} = 5.5$  TeV. This leads to a much higher initial energy density. Higher energy density and increased lifetime will make initial state effects less important, but will also enhance the role of the QGP phase over final state hadronic interactions. On the other hand, probes with very high transverse momentum, up to 100 GeV/c, will be available and it might be possible to measure jets [25]. Also heavy  $c$  and  $b$  quarks are plentiful probes at this energy.

### 4.1 Saturation physics

The relevance of saturation of the nuclear wave function [26] has already been discussed at lower energies. It is clear that LHC will be the ideal testing ground for saturation physics. The basic idea is that the gluon distribution in a QCD bound state cannot continuously grow fast at small Bjorken  $x$  without violating unitarity. At some point, gluon fusion will balance the growth. The scale at which the probability of gluon interactions in the nucleus wave function becomes of the order of one determines the saturation scale  $Q_s$  [26]

$$\frac{xG_A(x, Q_s^2)}{\pi R_A^2} \frac{\alpha_s(Q_s^2)}{Q_s^2} \sim 1. \quad (10)$$

From this equation one obtains the scaling with the nuclear size  $Q_s^2 \sim A^{1/3} x^{-0.5}$ . Starting from these assumptions various phenomenological consequences have been derived [27] for QCD at large  $\sqrt{s}$ . See e.g. [28] for an overview.

Saturation has also to be taken into account, when one of the fundamental questions is addressed: What are the particle multiplicities we can expect at LHC? This is very important for the detector design. Estimates have been given in [29] using perturbative QCD and saturation.

## 4.2 Jet quenching at the LHC

It is expected that the effect of jet quenching at LHC is even larger than at RHIC due to the higher energy density in the medium. Estimates depending on the produced particle multiplicity show that quenching factors of 10–30 can occur for pions at  $P_T = 10$  GeV [30]. Nevertheless, hard QCD will be an important part of the heavy ion program at LHC. It might be possible to measure jets directly, as it is done in  $p + \bar{p}$  and  $e^+ + e^-$  collisions. That eliminates the uncertainty coming from fragmentation functions in theoretical calculations and could be a valuable contribution to our understanding of energy loss in the medium [25].

## 4.3 Recombination at the LHC

The large nuclear suppression factor raises the question whether “soft” thermal physics will push its limits to even higher  $P_T$  at LHC. Preliminary studies with recombination from a thermalized parton phase confirm this. Figs. 5,6 shows an estimate of  $\pi^0$  and  $p$  spectra at LHC taking into account recombination and fragmentation [20]. The energy loss used is in accordance with the estimates of Gyulassy and Vitev [30] and for the thermal parton phase a temperature  $T = 175$  MeV and radial flow  $v_T = 0.75c$  are assumed. The crossover between the recombination domain and the pQCD domain is shifted to 6 GeV/ $c$  (from 4 GeV/ $c$  at RHIC [20]) for pions and to 8 GeV/ $c$  (from 6 GeV/ $c$  at RHIC) for protons. Correspondingly the  $p/\pi^0$  ratio at LHC is also shifted to higher  $P_T$ , see Fig. 7.

## 4.4 Measurements of medium properties

Once partonic energy loss is established, one would like to measure properties of the QGP by using hard QCD probes. One sort of precision measurements could be photon-tagged jets or hadrons. For this one considers the back-to-back production of a parton and a photon, e.g.  $q + g \rightarrow q + \gamma$  as shown in Fig. 8. Due to the weakness of electromagnetic interactions, the photon can leave the medium unaffected, while the outgoing parton will suffer from final state interactions. By momentum conservation the transverse momentum of the photon is equal to the initial momentum of the outgoing parton directly after the production. But the parton will suffer from energy loss before it can hadronize. By tagging a reference photon and looking at hadrons or jets at the opposite side, precision measurements of energy loss will be possible [31]. The same measurement can be done with back-to-back production of a parton and a virtual photon, which then decays into a lepton pair [32].

Another promising idea is to measure induced photon radiation from fast partons interacting with the medium [33]. It is characteristic for the Born cross

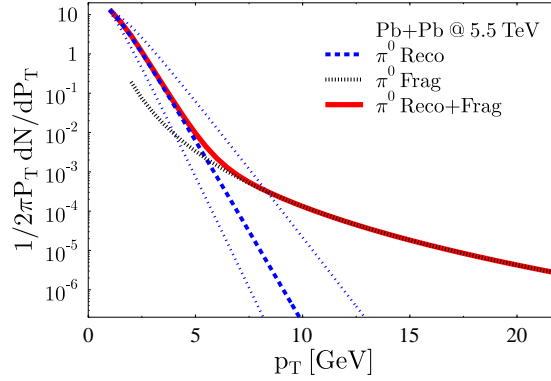


**Fig. 5.** Transverse momentum spectra of  $\pi^0$  for central Pb+Pb collisions with  $\sqrt{s} = 5.5$  GeV at midrapidity. Fragmentation from pQCD (dotted), recombination (long dashed) and the sum of both (solid line) are shown. The parameters for the thermal parton phase are  $T = 175$  MeV and  $v_T = 0.75c$ . For pions recombination for different radial flow velocities  $0.65c$  and  $0.85c$  (short dashed, from below) are also shown.

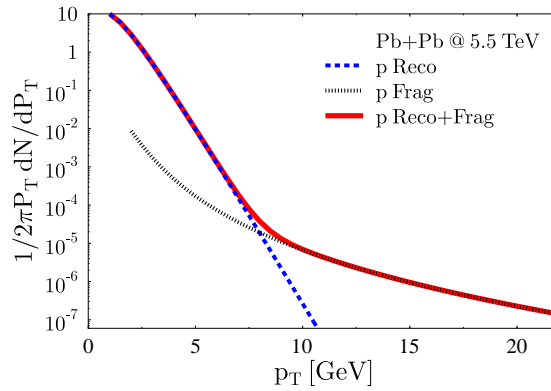


**Fig. 6.** The same as Fig. 5 for the transverse momentum spectrum of protons ( $v_T = 0.75c$  only).

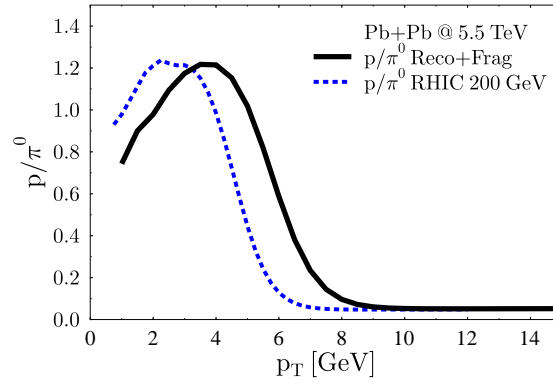


**Fig. 7.** The  $p/\pi^0$  ratio for Pb+Pb at LHC (solid) and for Au+Au at RHIC (dashed line) as predicted by a calculation using recombination and pQCD. The baryon enhancement is pushed to higher  $P_T$  for LHC.

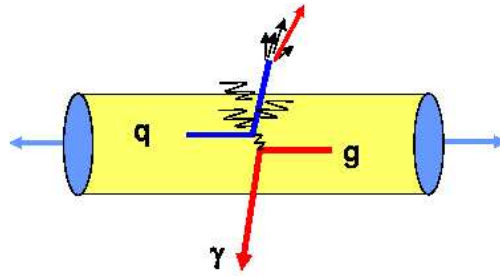


**Fig. 8.** Tagging of a jet or leading hadron by a photon on the other side: The photon can escape without final state interactions and carries information about the transverse momentum of the simultaneously produced parton before that loses energy in the medium.

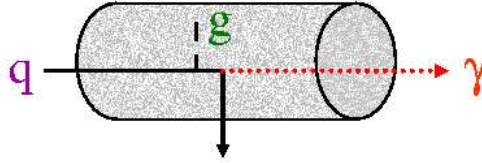


**Fig. 9.** Jet photon conversion: A fast parton is turned into a photon with comparable momentum by interactions with the medium.

sections for these processes, e.g.

$$q(\text{jet}) + \bar{q}(\text{medium}) \rightarrow g + \gamma \text{ or } q(\text{jet}) + g(\text{medium}) \rightarrow q + \gamma, \quad (11)$$

— see Fig. 9 — that they peak in forward and backward directions (in the center of mass frame). That means that the three-momentum of the photon is very close to one of the two initial momenta. If one restricts the measurement of the photon to large transverse momentum, say  $P_T > 4 \text{ GeV}/c$ , then the momentum of the photon will be that of the fast parton. This jet-photon conversion mechanism is another opportunity to measure the momentum of a fast parton in the plasma. This time the photon emission will take place while this parton is traveling through the plasma and, in order to obtain the photon rate, one has to integrate over the path of the parton. Therefore this measurement is sensitive to the evolution of density and temperature of the medium. It has been estimated that photons from this conversion mechanism are shining quite brightly at RHIC and LHC compared to other photon sources, cf. Fig. 10. Again, similar measurements are possible with dileptons instead of photons [34].

## 5 Summary

We have discussed several key issues of heavy ion physics. While we might already discover the quark gluon plasma at RHIC, it will be at LHC that we can systematically study its properties by making use of the plentiful hard probes. Some important questions have to be addressed.

- How does gluon saturation work at small  $x$ ?
- How exactly are fragmentation functions modified in the medium?
- How does the energy loss depend on the energy density?
- Are heavy quarks thermalized?
- What is the role of nuclear higher twist effects?

The LHC will be the ideal machine to provide answers.

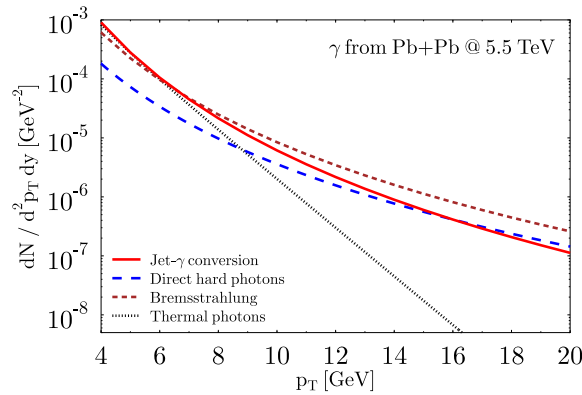


**Fig. 10.** Photons from jet-photon conversion (solid line) at LHC compared to other direct photon sources: thermal radiation from the plasma (dotted), direct photons from primary hard interactions (long dashed) and bremsstrahlung from primary hard interactions (short dashed line). The yield from conversion is of the same order of magnitude as the other processes. See [33] for further details.

## References

1. F. Karsch, Nucl. Phys. A **698**, 199 (2002).
2. F. Karsch, Lect. Notes Phys. **583**, 209 (2002), hep-lat/0106019.
3. Z. Fodor and S. D. Katz, JHEP **0203**, 014 (2002)
4. E. Schnedermann, J. Sollfrank and U. W. Heinz, Phys. Rev. C **48**, 2462 (1993).
5. J. Rafelski and B. Müller, Phys. Rev. Lett. **48**, 1066 (1982); Erratum *ibid.* **56**, 2334 (1986).
6. K. Fanebust *et al.* [NA57 Collaboration], J. Phys. G **28**, 1607 (2002).
7. T. Matsui and H. Satz, Phys. Lett. B **178**, 416 (1986).
8. O. Kaczmarek, F. Karsch, P. Petreczky and F. Zantow, Phys. Lett. B **543**, 41 (2002).
9. R. Rapp and E. V. Shuryak, Phys. Rev. D **67**, 074036 (2003); R. L. Thews, hep-ph/0305316.
10. J. D. Bjorken, FERMILAB-PUB-82-059-THY (1982).
11. M. H. Thoma and M. Gyulassy, Nucl. Phys. B **351**, 491 (1991); X. N. Wang and M. Gyulassy, Phys. Rev. Lett. **68**, 1480 (1992); M. Gyulassy and X. Wang, Nucl. Phys. B **420**, 583 (1994); R. Baier, Y. L. Dokshitzer, A. H. Mueller, S. Peigne and D. Schiff, Nucl. Phys. B **483**, 291 (1997); B. G. Zakharov, JETP Lett. **65**, 615 (1997); M. Gyulassy, P. Levai and I. Vitev, Phys. Rev. Lett. **85**, 5535 (2000); U. A. Wiedemann, Nucl. Phys. B **588**, 303 (2000); R. Baier, Y. L. Dokshitzer, A. H. Mueller and D. Schiff, JHEP **0109**, 033 (2001).
12. K. Adcox *et al.* [PHENIX Collaboration], Phys. Rev. Lett. **88**, 022301 (2002); C. Adler *et al.* [STAR Collaboration], Phys. Rev. Lett. **90**, 082302 (2003).
13. S. S. Adler *et al.* [PHENIX Collaboration], nucl-ex/0304022.
14. S. S. Adler *et al.* [PHENIX Collaboration], nucl-ex/0306021; J. Adams *et al.* [STAR Collaboration], nucl-ex/0306024.
15. X. F. Guo and X. N. Wang, Phys. Rev. Lett. **85**, 3591 (2000); Nucl. Phys. A **696**, 788 (2001); E. Wang and X. N. Wang, Phys. Rev. Lett. **89**, 162301 (2002).

16. L. D. Landau and I. Pomeranchuk, Dokl. Akad. Nauk Ser. Fiz. **92**, 535 (1953); *ibid.* **92**, 735 (1953); A. B. Migdal, Phys. Rev. **103**, 1811 (1956).
17. S. S. Adler *et al.* [PHENIX Collaboration], nucl-ex/0305036.
18. J. Adams *et al.* [STAR Collaboration], nucl-ex/0306007.
19. K. P. Das and R. C. Hwa, Phys. Lett. B **68**, 459 (1977); Erratum *ibid.* **73**, 504 (1978); R. J. Fries, B. Müller, C. Nonaka and S. A. Bass, Phys. Rev. Lett. **90**, 202303 (2003); V. Greco, C. M. Ko and P. Levai, Phys. Rev. Lett. **90**, 202302 (2003); R. C. Hwa and C. B. Yang, Phys. Rev. C **67**, 034902 (2003).
20. R. J. Fries, B. Müller, C. Nonaka and S. A. Bass, nucl-th/0306027.
21. J. Adams *et al.* [STAR Collaboration], nucl-ex/0305015.
22. J. Velkovska for the PHENIX Collaboration, Talk at SQM2003, J. Phys. G *to be published*.
23. Z. W. Lin and C. M. Ko, Phys. Rev. Lett. **89**, 202302 (2002); S. A. Voloshin, Nucl. Phys. A **715**, 379c (2003).
24. S. S. Adler *et al.* [PHENIX Collaboration], nucl-ex/0305013; P. Sorensen for the STAR Collaboration, nucl-ex/0305008.
25. CERN Yellow Report on “Hard probes in heavy collisions at LHC”, *to appear* (2003).
26. L. V. Gribov, E. M. Levin and M. G. Ryskin, Nucl. Phys. B **188**, 555 (1981); A. H. Mueller and J. W. Qiu, Nucl. Phys. B **268**, 427 (1986); J. P. Blaizot and A. H. Mueller, Nucl. Phys. B **289**, 847 (1987).
27. L. D. McLerran and R. Venugopalan, Phys. Rev. D **49**, 2233 (1994); *ibid.* **49**, 3352 (1994); J. Jalilian-Marian, A. Kovner, L. D. McLerran and H. Weigert, Phys. Rev. D **55**, 5414 (1997).
28. E. Iancu, A. Leonidov and L. McLerran, hep-ph/0202270.
29. K. J. Eskola, K. Kajantie, P. V. Ruuskanen and K. Tuominen, Nucl. Phys. B **570**, 379 (2000).
30. I. Vitev and M. Gyulassy, Phys. Rev. Lett. **89**, 252301 (2002).
31. X. N. Wang, Z. Huang and I. Sarcevic, Phys. Rev. Lett. **77**, 231 (1996).
32. D. K. Srivastava, C. Gale and T. C. Awes, Phys. Rev. C **67**, 054904 (2003).
33. R. J. Fries, B. Müller and D. K. Srivastava, Phys. Rev. Lett. **90**, 132301 (2003).
34. D. K. Srivastava, C. Gale and R. J. Fries, Phys. Rev. C **67**, 034903 (2003).